PROCEEDINGS OF SCIENCE

Constraints on upward-going air showers using the Pierre Auger Observatory data

Emanuele De Vito[a,b,*] **for the Pierre Auger Collaboration**[c], **Remy Prechelt**[d], **Andrés Romero-Wolf**[e], **Stephanie Wissel**[f] **and Andrew Zeolla**[g]

[a] *Università del Salento, Dipartimento di Matematica e Fisica "E. De Giorgi", Lecce, Italy*
[b] *INFN, Sezione di Lecce, Lecce, Italy*
[c] *Observatorio Pierre Auger, Av. San Martín Norte 304, 5613 Malargüe, Argentina*
Full author list: https://www.auger.org/archive/authors_icrc_2023.html
[d] *University of Hawaii, Hawaii, USA*
[e] *Caltech Jet Propulsion Laboratory, Pasadena, California, USA*
[f] *California Polytechnic State University, San Luis Obispo, California, USA*
[g] *Pennsylvania State University, University Park, Pennsylvania, USA*

E-mail: spokespersons@auger.org

The fluorescence detector (FD) of the Pierre Auger Observatory is sensitive to upward-going air showers with energies above 10^{17} eV. Given its operation time and wide field of view, the FD has the potential to support or constrain the "anomalous" observations by the ANITA detector, interpreted as upward-going air showers that would be indicative of Beyond Standard Model (BSM) physics. To this end, a search for upward-going air showers with the FD has been performed applying selection criteria that were optimized using 10% of FD data. Dedicated background simulations (downward-going events) have been performed to estimate our capability to distinguish candidates from false positives. Also dedicated signal simulations (upward-going events) have been used to estimate our sensitivity to such showers with a focus on the energy region close to the ANITA observations.

Improved and updated results of the Pierre Auger Observatory exposure to upward-going showers will be presented after the unblinding of 14 years of FD data. Extensive simulations allow the FD exposure to be obtained at lower energies which are particularly relevant for the comparison with the ANITA results. A refinement of the method for signal discrimination and background rejection has also been applied. The implications are discussed under the assumption that the ANITA events were due to upward-going events.

38th International Cosmic Ray Conference (ICRC2023)
26 July – 3 August, 2023
Nagoya, Japan

*Speaker

PoS(ICRC2023)1099

1. Introduction

The Fluorescence Detector (FD) of the Pierre Auger Observatory consists of multiple telescopes that collect the fluorescence light emitted by the air as showers, induced by cosmic rays, develop in the atmosphere. The FD is also sensitive to upward-going cosmic-ray-like air showers which are of particular interest after the ANITA Collaboration reported the observation of two "anomalous" events [1, 2]. During its first and third flight, the balloon experiment detected two events with elevation angles of $27.4^\circ \pm 0.3^\circ$ and $35.0^\circ \pm 0.3^\circ$ respectively, and energies above ~ 0.2 EeV [3]. The energies and elevation angles are hard to reconcile with the predictions of the standard model of particle physics, so a confirmation or a constraint from a different experiment would be of particular interest.

To this end, the Pierre Auger Collaboration has performed a search for cosmic-ray-like upward-going air showers with the FD in 14 years of data collected between 2004 and 2018. Signal simulations have been studied to estimate the FD sensitivity to upward-going air showers distributed in the energy and zenith angle regions of interest. The potential background from downward-going cosmic rays, erroneously reconstructed as upward-going, has been estimated with extensive simulations as well. A 10% fraction of the available data has been used to identify and remove the background of untagged upward-going lasers used by the Collaboration to monitor the atmosphere. These cuts together with those defined using simulations have been applied to calculate the expected background in the full data sample and to search for candidates in the data. The FD exposure has also been calculated and the Auger result after the unblinding has been compared with the fluxes inferred from the ANITA observations.

2. Signal simulation

Upward-going air showers could be produced as an outcome of an upward-going particle emerging from the Earth crust and interacting or decaying in the atmosphere at a certain height or just below the Earth crust. For zenith angles above the Earth skimming limit ($\theta > 95^\circ$), they are unlikely to trigger the Surface Detector (SD) of the Pierre Auger Observatory, whereas the FD can observe the shower development in the atmosphere. To calculate the FD exposure, upward-going air showers have been simulated with CONEX [4] and reconstructed within the Offline Framework [5]. The FD has negligible detection efficiency below $10^{16.5}$ eV, therefore this analysis has been limited to showers with $\log_{10}(E/\text{eV}) \in [16.5, 19]$. Simulations have been made according to an energy distribution of E^{-1} and assuming an isotropic distribution of events. The zenith angles have been sampled within $\theta \in [110^\circ, 180^\circ]$ (elevation angles in $[20^\circ, 90^\circ]$). The impact points of the particle trajectory on the ground, later referred as "exit points", have been sampled in a square of 100×100 km^2 centered at the SD station closest to the center of the SD array. The exit points can also be located behind the field of view of a telescope, since the generation area extends up to ~20 km behind each FD site. The height of the first interaction point (h) is also a relevant parameter when simulating upward-going events as showers starting high in the atmosphere tend to be further away and are less likely to trigger the data acquisition. Showers have been uniformly generated with $h \in [0, 9]$ km above the ground altitude of the Observatory (~1400 m a.s.l). A single proton has been used as primary particle because it can be easily adapted to fit other interesting

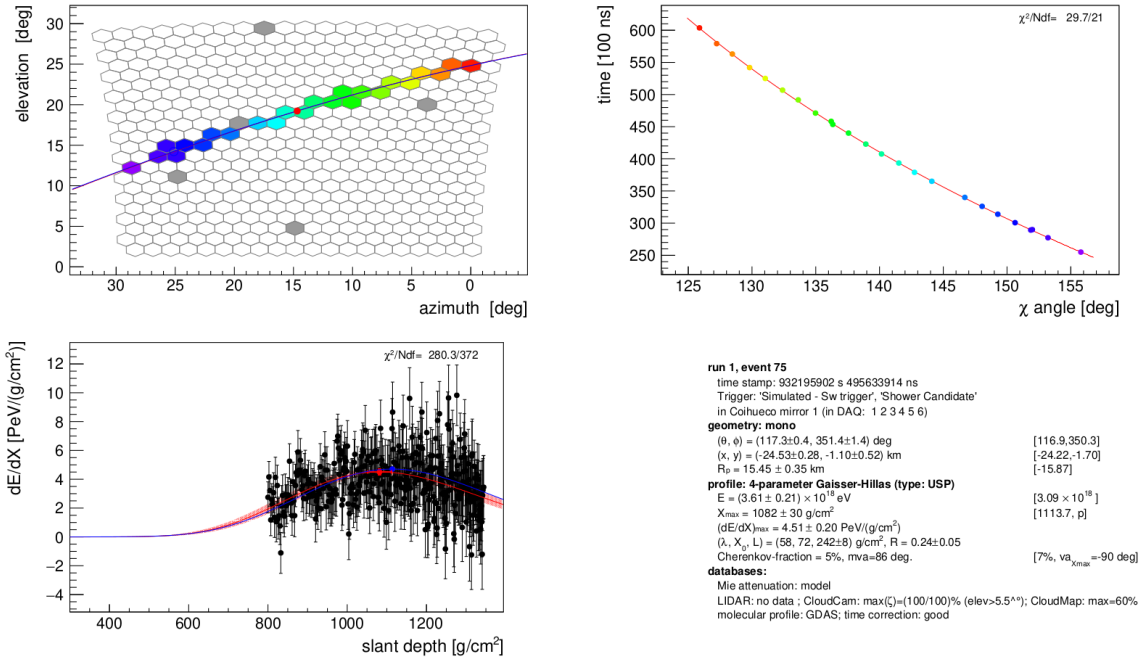

Figure 1: Event display of an upward-going proton induced shower simulated with CONEX and reconstructed with the Offline. The top left panel shows the activated pixels on the camera, with their arrival time as a function of their elevation on the top right panel. The reconstructed longitudinal profile of the shower is displayed in the bottom left panel, while the parameters from the reconstruction are reported in the bottom right panel with true simulated values within square brackets. The colors in the top left and top right panels refer to the arrival time of the light (blue for early pixels, red for late pixels). The blue lines are for the Monte Carlo truth.

scenarios [6]. Sibyll 2.3c [7, 8] and UrQMD 1.3 [9] have been used as hadronic models at high and low energies, respectively. A time dependent detector simulation has been used to take into account all the FD configurations and their time variability during the 14 years of operation used for the analysis [10]. In total, 6.5×10^7 upward-going showers have been simulated in the aforementioned energy range aiming in particular at increasing the number of simulated events below $10^{17.5}$ eV. This represents an important step forward with respect to the previous analysis [11] as it allows extending the calculation of the FD detection efficiency down to 10^{17} eV that is the most relevant energy region for the comparison with ANITA. Figure 1 shows a simulated upward-going proton as seen in the Offline event display [5]. The activated pixels on the camera are shown on the top left panel, while their arrival times are plotted on the top right panel as a function of the elevation angle in the plane containing both the detector and the shower axis (i.e. Shower Detector Plane, SDP). The reconstructed longitudinal profile is displayed in the bottom left panel, while the reconstructed parameters are reported in the bottom right panel. For reference, the true values are also reported within square brackets.

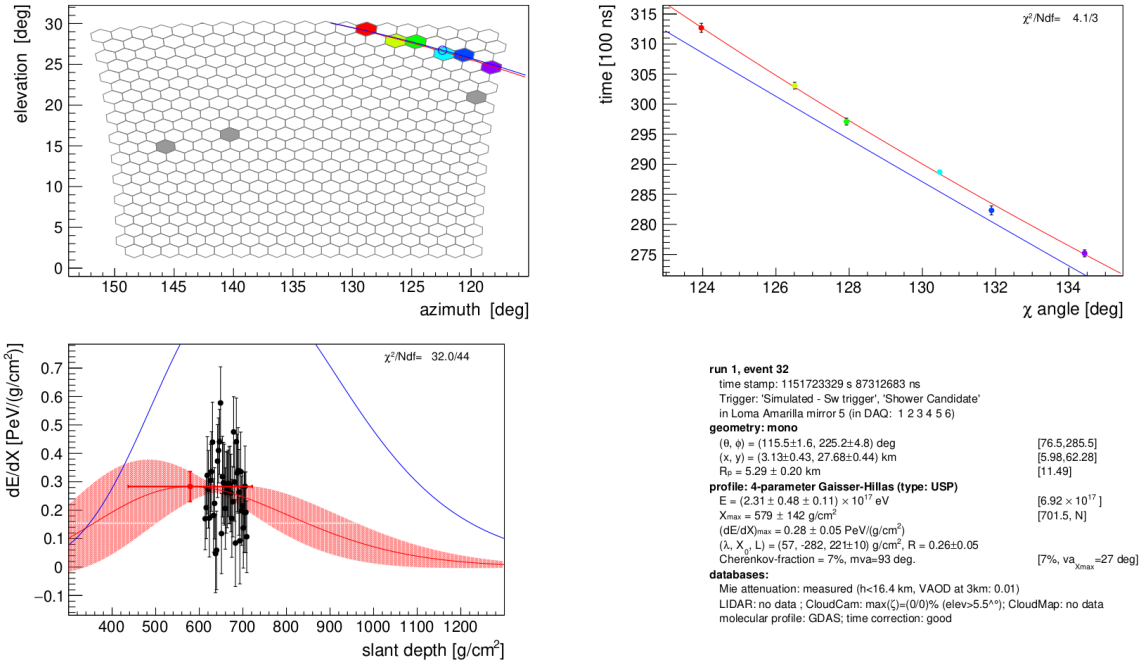

Figure 2: Event display of a simulated downward-going event with a zenith angle of 76.5° and reconstructed as an upward-going shower ($\theta = 115.5°$). The blue lines are for the Monte Carlo truth.

3. Background simulation

In this analysis no SD data is required, as upward-going air showers generally can not trigger the stations. In absence of any signal from the SD, downward-going events with specific geometries can be incorrectly reconstructed as upward-going and vice-versa. As seen in [11], for pure geometrical reasons, the signal of an event whose impact point is located behind the telescope can mimic an upward-going event. Therefore, dedicated and extensive simulations of downward-going events have been used to study the cosmic ray background.

Helium, nitrogen an iron nuclei, as well as protons, have been considered as primary particles with $\log_{10}(E/\text{eV}) \in [17, 20]$ and zenith angle $\theta \in [0°, 90°]$. As for signal simulations, Sybill2.3c and UrQMD 1.3 have been used as hadronic interaction models for high and low energies respectively. The overall number of simulated shower for the background is $\sim 2.5 \times 10^8$. Signal and background simulations along with data have been exploited to define selection criteria to distinguish signal events from false positives. Figure 2 shows an example of a downward-going event simulated at $\theta \sim 76°$ reconstructed as upward-going with an elevation angle of $\sim 25°$ ($\theta \sim 115°$).

4. Data cleaning and selection criteria

The FD observes the shower development in the atmosphere. Since any variation in temperature, humidity, pressure or aerosol concentration may influence the shower evolution, it is very important to have a continuous monitoring of the atmospheric conditions over the Observatory. To this end, millions of laser pulses are fired from different positions during nights of data taking [12]. These shots are usually recorded and stored so they can be easily removed during the analysis.

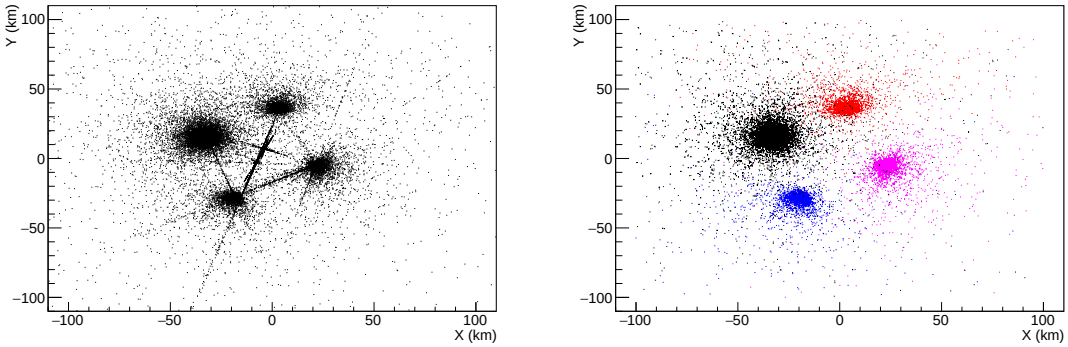

Figure 3: Distribution of the exit point of the events in the burn sample before (left) and after (right) the laser identification and rejection. The straight lines, related to laser events, are correctly removed and only clusters of events remained close to each of the FD sites.

However some lasers may have not been properly labelled producing false positives. A sample of 10% of the available FD data ("burn sample") has been used to identify and remove these events by exploiting the firing frequencies and the known laser locations inside the array. Figure 3 left shows the exit points for the events of the burn sample in which lasers tend to accumulate along straight-line patterns. That is because lasers typically share the same SDP which is reconstructed with high accuracy, unlike the reconstruction of the exit points witin the SDP which is less precise and creates these patterns. The right panel shows the same distribution after their identification and rejection. The colour scheme identifies which FD site triggered on each specific event.

To improve the discrimination between signal and background events, both data and simulations have been reconstructed using a procedure named as Profile Constrained Geometry Fit Reconstruction (PCGF) [13]. Unlike the standard reconstruction method, which finds the best geometry and the shower longitudinal profile in two separate steps, the PCGF reconstruction uses a single likelihood maximization to fit both the arrival time sequence and the light profile at the same time. The PCGF can also run in two separate modes, referred as PCGFdown and PCGFup, with zenith angle limited between $[0°, 90°]$ and $[90°, 180°]$ respectively. This results in two independent values of the maximum likelihoods, L_{down} and L_{up}, that can be compared to discriminate between events that are more likely to be downward-going ($L_{\text{down}} > L_{\text{up}}$) and vice-versa. The most precise geometrical reconstruction has been proven to be associated to a smooth maximum in the combined likelihood. As an improvement to the previous analysis [11], this approach has been used for L_{up}, while, to be conservative, an absolute maximum in the likelihood is accepted for L_{down} as done in the past.

Quality selection criteria have been applied to guarantee a minimum reconstruction quality while keeping enough statistics. This includes requiring $\theta > 110°$, clean atmosphere, low cloud coverage, at least five pixels in a compact pattern and an observed longitudinal profile of at least $80\,\text{g}\,\text{cm}^{-2}$. Moreover, all events without a successful upward reconstruction are excluded from this analysis. Then a new variable has been defined as

$$l = \frac{\arctan(-2\log(L_{\text{down}}/\max(L_{\text{down}}, L_{\text{up}}))/50)}{\pi/2}. \tag{1}$$

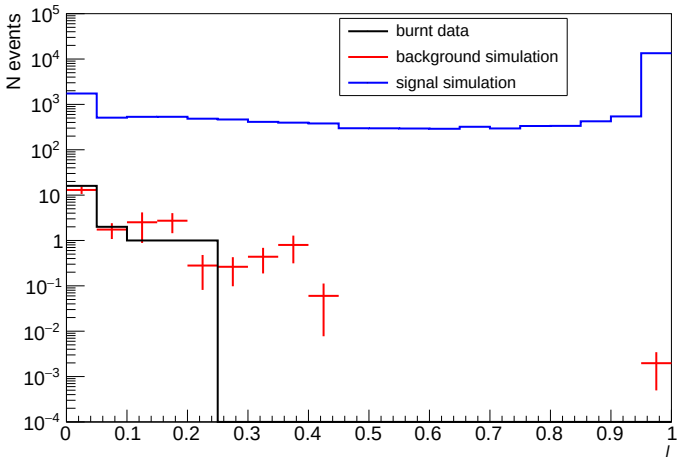

Figure 4: Distribution of l for background simulations (red), signal simulations (blue) and burn data sample (black). Background simulations have been weighted and normalized to the cosmic ray spectrum and rescaled to the burn sample fraction, while signal simulations have not been weighted.

According to this definition $l = 0$ if $L_{\text{down}} > L_{\text{up}}$, $l \to 1$ if $L_{\text{up}} \gg L_{\text{down}}$ and $l = 1$ if no downward reconstruction is found for that specific event. Figure 4 shows the distribution of this variable for the burn data sample (black), signal simulation (blue) and background simulation (red). Background simulations have been weighted and normalized to the observed cosmic ray spectrum [14] and were rescaled to the burn sample fraction.

The background distribution has been fitted with an exponential function and the cut value on l has been chosen as the value that minimizes the integral upper limit which can be set in case no candidates are found in the full data sample after the unblinding, according to the procedure described in [11]. The cut value to discriminate between candidate and background events is set at $l = 0.55$ as in the previous analysis, but the expected background after the unblinding is now $n_{\text{bkg}} = 0.27 \pm 0.12$ as a result of the general refinement of the reconstruction described above.

5. Results

Following the steps described in [11], the FD exposure for upward-going air showers can be calculated. Figure 5 left shows the double differential exposure as a function of the shower energy and the height of first interaction, while the exposure integrated in height is shown as a function of the energy in the right panel, calculated also for three different zenith sub-ranges. As a consequence of the extended simulation campaign described in Section 2, the exposure extends now down to 10^{17} eV.

After the unblinding of data one event passes all the selection criteria, which is consistent with the expected background. A preliminary integral upper limit to the flux of upward-going air showers can be set at

$$\begin{aligned} F^{95\%}_{\gamma=1}(E > 10^{17}\,\text{eV}) &= (7.2 \pm 0.2) \cdot 10^{-21}\,\text{cm}^{-2}\text{sr}^{-1}\text{s}^{-1} \\ F^{95\%}_{\gamma=2}(E > 10^{17}\,\text{eV}) &= (3.6 \pm 0.2) \cdot 10^{-20}\,\text{cm}^{-2}\text{sr}^{-1}\text{s}^{-1} \end{aligned} \tag{2}$$

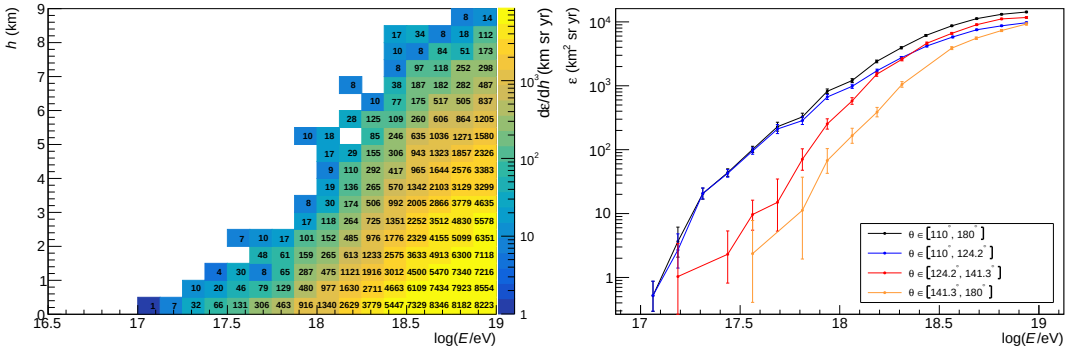

Figure 5: (Left) FD double differential exposure for upward-going air showers as a function of the shower energy and the height of the first interaction point for $\theta \in [110°, 180°]$. (Right) FD exposure as a function of the energy calculated for the whole zenith range in black and for three different sub-ranges: $\theta \in [110°, 124.2°]$ in blue, $\theta \in [124.2°, 141.3°]$ in red, $\theta \in [141.3°, 180°]$ in orange

at 95% CL by weighting the exposure with two different spectral indices $\gamma = 1, 2$. Given that the exposure calculation has been extended at lower energies, the upper limits are now provided above 10^{17} eV.

In a joint effort with members of the ANITA Collaboration, it has been possible to analytically evaluate the exposure of ANITA for the two "anomalous" events with $\theta \in [110°, 130°]$ and $\log(E/\text{eV}) \in [17, 18.5]$. The events have been observed during the first (ANITA I) and the third (ANITA III) flights with a lower threshold and an upgraded apparatus being used for the latter. Therefore the Auger and ANITA results have been compared separately for the two events. Figure 6 shows a comparison of the Auger integral upper bound (in blue) with the ANITA inferred flux (in red) or 95% CL upper limit (light red) for both ANITA I and ANITA III events on the left and right side respectively. All the limits have been calculated within the same energy and zenith sub-ranges given by ANITA. The comparison has been done for both $\gamma = 1, 2$ with the Auger limit being 2 orders of magnitude lower in case of an E^{-1} energy spectrum and at ~ 30 times lower in case of a E^{-2} spectrum.

6. Conclusion

A search for upward-going air showers has been performed with the FD of the Pierre Auger Observatory using data collected in 14 years of operation between 2004 and 2018. Signal and background simulations have been used to study the FD potential to distinguish between signal events and false positives. A 10% fraction of the data sample has been used to identify and reject lasers from data. Further quality selection criteria have been applied and a new variable l has been defined to discriminate between upward and downward-going showers. After unblinding, only one event has passed this cut, compatible with the expected background of 0.27 ± 0.12 events. Signal simulations have been used to calculate the FD exposure for upward-going showers and an integral upper limit has been set for two different spectral indices $\gamma = 1, 2$. An analytical evaluation of the ANITA exposures for the two anomalous events has been used to compare the Auger upper limits

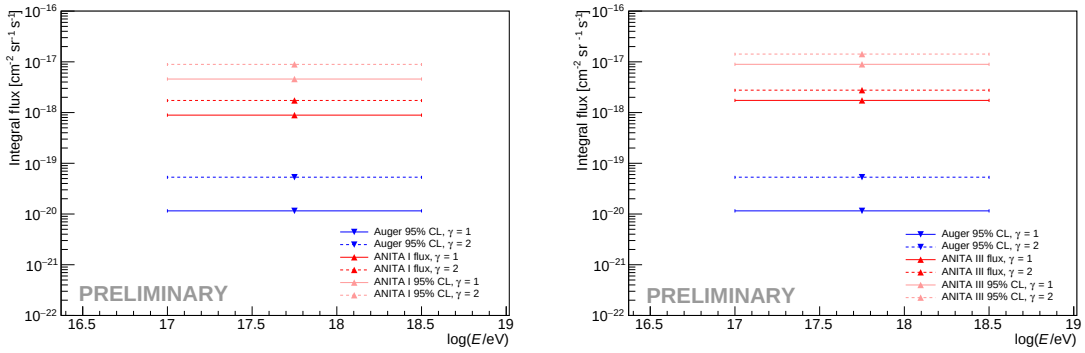

Figure 6: (Left) Comparison of Auger upper limits with the inferred ANITA I flux in red and ANITA I 95% CL upper limit in case of $\gamma = 1, 2$. (Right) Comparison of Auger upper limits with ANITA III event. All the limits have been calculated within the same zenith and energy sub-ranges ($\theta \in [110°, 130°]$ and $\log(E/\text{eV}) \in [17, 18.5]$).

with the inferred ANITA fluxes. For both events the Auger limits are found to be two orders of magnitude lower than the ANITA flux in case of $\gamma = 1$ and about 30 times lower in case of $\gamma = 2$.

References

[1] P. W. Gorham *et al.* [ANITA Coll.], *Phys. Rev. Lett.* **117** (2016) 071101. [1603.05218]

[2] P. W. Gorham *et al.* [ANITA Coll.], *Phys. Rev. Lett.* **121** (2018) 161102. [1803.05088]

[3] A. Romero-Wolf, S. A. Wissel, H. Schoorlemmer, W. R. Carvalho, J. Alvarez-Muñiz, E. Zas, P. Allison, O. Banerjee, L. Batten and J. J. Beatty, *et al.*, *Phys. Rev. D* **99** (2019) 063011. [1811.07261]

[4] T. Bergmann, R. Engel, D. Heck, N. N. Kalmykov, S. Ostapchenko, T. Pierog, T. Thouw and K. Werner, *Astropart. Phys.* **26** (2007) 420-432. [astro-ph/0606564]

[5] S. Argiro, S. L. C. Barroso, J. Gonzalez, L. Nellen, T. C. Paul, T. A. Porter, L. Prado, Jr., M. Roth, R. Ulrich and D. Veberic, *Nucl. Instrum. Meth. A* **580** (2007) 1485-1496. [0707.1652]

[6] B. Yue *et al.* [Pierre Auger Coll.], *Proc. 38th Int. Cosmic Ray Conf., Nagoya, Japan (2023)*, PoS(ICRC2023)1095.

[7] F. Riehn, H. P. Dembinski, R. Engel, A. Fedynitch, T. K. Gaisser and T. Stanev, *Proc. 35th Int. Cosmic Ray Conf., Busan, Korea (2017)*, PoS(ICRC2017)301. [1709.07227]

[8] E. J. Ahn, R. Engel, T. K. Gaisser, P. Lipari and T. Stanev, *Phys. Rev. D* **80** (2009) 094003. [0906.4113]

[9] S. A. Bass, M. Belkacem, M. Bleicher, M. Brandstetter, L. Bravina, C. Ernst, L. Gerland, M. Hofmann, S. Hofmann and J. Konopka, et al. *Prog. Part. Nucl. Phys.* **41** (1998) 255-369. [nucl-th/9803035]

[10] P. Abreu *et al.* [Pierre Auger Coll.], *Astropart. Phys.* **34** (2011) 368-381. [1010.6162]

[11] M. Mastrodicasa *et al.* [Pierre Auger Coll.], *Proc. 37th Int. Cosmic Ray Conf., Berlin, German (2021)*, PoS(ICRC2021)1140.

[12] A. Aab *et al.* [Pierre Auger Coll.], *Nucl. Instrum. Meth. A* **798** (2015) 172-213. [1502.01323]

[13] V. Novotny *et al.* [Pierre Auger Coll.], *Proc. 36th Int. Cosmic Ray Conf., Madison, WI, U.S.A. (2019)*, PoS(ICRC2019)374. [1909.09073]

[14] A. Aab *et al.* [Pierre Auger Coll.], Phys. Rev. Lett. **125** (2020) 121106. [2008.06488]

The Pierre Auger Collaboration

A. Abdul Halim[13], P. Abreu[72], M. Aglietta[54,52], I. Allekotte[1], K. Almeida Cheminant[70], A. Almela[7,12], R. Aloisio[45,46], J. Alvarez-Muñiz[79], J. Ammerman Yebra[79], G.A. Anastasi[54,52], L. Anchordoqui[86], B. Andrada[7], S. Andringa[72], C. Aramo[50], P.R. Araújo Ferreira[42], E. Arnone[63,52], J. C. Arteaga Velázquez[67], H. Asorey[7], P. Assis[72], G. Avila[11], E. Avocone[57,46], A.M. Badescu[75], A. Bakalova[32], A. Balaceanu[73], F. Barbato[45,46], A. Bartz Mocellin[85], J.A. Bellido[13,69], C. Berat[36], M.E. Bertaina[63,52], G. Bhatta[70], M. Bianciotto[63,52], P.L. Biermann[h], V. Binet[5], K. Bismark[39,7], T. Bister[80,81], J. Biteau[37], J. Blazek[32], C. Bleve[36], J. Blümer[41], M. Boháčová[32], D. Boncioli[57,46], C. Bonifazi[8,26], L. Bonneau Arbeletche[21], N. Borodai[70], J. Brack[j], P.G. Brichetto Orchera[7], F.L. Briechle[42], A. Bueno[78], S. Buitink[15], M. Buscemi[47,61], M. Büsken[39,7], A. Bwembya[80,81], K.S. Caballero-Mora[66], S. Cabana-Freire[79], L. Caccianiga[59,49], I. Caracas[38], R. Caruso[58,47], A. Castellina[54,52], F. Catalani[18], G. Cataldi[48], L. Cazon[79], M. Cerda[10], A. Cermenati[45,46], J.A. Chinellato[21], J. Chudoba[32], L. Chytka[33], R.W. Clay[13], A.C. Cobos Cerutti[6], R. Colalillo[60,50], A. Coleman[90], M.R. Coluccia[48], R. Conceição[72], A. Condorelli[37], G. Consolati[49,55], M. Conte[56,48], F. Convenga[41], D. Correia dos Santos[28], P.J. Costa[72], C.E. Covault[84], M. Cristinziani[44], C.S. Cruz Sanchez[3], S. Dasso[4,2], K. Daumiller[41], B.R. Dawson[13], R.M. de Almeida[28], J. de Jesús[7,41], S.J. de Jong[80,81], J.R.T. de Mello Neto[26,27], I. De Mitri[45,46], J. de Oliveira[17], D. de Oliveira Franco[21], F. de Palma[56,48], V. de Souza[19], E. De Vito[56,48], A. Del Popolo[58,47], O. Deligny[34], N. Denner[32], L. Deval[41,7], A. di Matteo[52], M. Dobre[73], C. Dobrigkeit[21], J.C. D'Olivo[68], L.M. Domingues Mendes[72], J.C. dos Anjos, R.C. dos Anjos[25], J. Ebr[32], F. Ellwanger[41], M. Emam[80,81], R. Engel[39,41], I. Epicoco[56,48], M. Erdmann[42], A. Etchegoyen[7,12], C. Evoli[45,46], H. Falcke[80,82,81], J. Farmer[89], G. Farrar[88], A.C. Fauth[21], N. Fazzini[e], F. Feldbusch[40], F. Fenu[41,d], A. Fernandes[72], B. Fick[87], J.M. Figueira[7], A. Filipčič[77,76], T. Fitoussi[41], B. Flaggs[90], T. Fodran[80], T. Fujii[89,f], A. Fuster[7,12], C. Galea[80], C. Galelli[59,49], B. García[6], C. Gaudu[38], H. Gemmeke[40], F. Gesualdi[7,41], A. Gherghel-Lascu[73], P.L. Ghia[34], U. Giaccari[48], M. Giammarchi[49], J. Glombitza[42,g], F. Gobbi[10], F. Gollan[7], G. Golup[1], M. Gómez Berisso[1], P.F. Gómez Vitale[11], J.P. Gongora[11], J.M. González[1], N. González[7], I. Goos[1], D. Góra[70], A. Gorgi[54,52], M. Gottowik[79], T.D. Grubb[13], F. Guarino[60,50], G.P. Guedes[22], E. Guido[44], S. Hahn[39], P. Hamal[32], M.R. Hampel[7], P. Hansen[3], D. Harari[1], V.M. Harvey[13], A. Haungs[41], T. Hebbeker[42], C. Hojvat[e], J.R. Hörandel[80,81], P. Horvath[33], M. Hrabovský[33], T. Huege[41,15], A. Insolia[58,47], P.G. Isar[74], P. Janecek[32], J.A. Johnsen[85], J. Jurysek[32], A. Kääpä[38], K.H. Kampert[38], B. Keilhauer[41], A. Khakurdikar[80], V.V. Kizakke Covilakam[7,41], H.O. Klages[41], M. Kleifges[40], F. Knapp[39], N. Kunka[40], B.L. Lago[16], N. Langner[42], M.A. Leigui de Oliveira[24], Y Lema-Capeans[79], V. Lenok[39], A. Letessier-Selvon[35], I. Lhenry-Yvon[34], D. Lo Presti[58,47], L. Lopes[72], L. Lu[91], Q. Luce[39], J.P. Lundquist[76], A. Machado Payeras[21], M. Majercakova[32], D. Mandat[32], B.C. Manning[13], P. Mantsch[e], S. Marafico[34], F.M. Mariani[59,49], A.G. Mariazzi[3], I.C. Mariş[14], G. Marsella[61,47], D. Martello[56,48], S. Martinelli[41,7], O. Martínez Bravo[64], M.A. Martins[79], M. Mastrodicasa[57,46], H.J. Mathes[41], J. Matthews[a], G. Matthiae[62,51], E. Mayotte[85,38], S. Mayotte[85], P.O. Mazur[e], G. Medina-Tanco[68], J. Meinert[38], D. Melo[7], A. Menshikov[40], C. Merx[41], S. Michal[33], M.I. Micheletti[5], L. Miramonti[59,49], S. Mollerach[1], F. Montanet[36], L. Morejon[38], C. Morello[54,52], A.L. Müller[32], K. Mulrey[80,81], R. Mussa[52], M. Muzio[88], W.M. Namasaka[38], S. Negi[32], L. Nellen[68], K. Nguyen[87], G. Nicora[9], M. Niculescu-Oglinzanu[73], M. Niechciol[44], D. Nitz[87], D. Nosek[31], V. Novotny[31], L. Nožka[33], A Nucita[56,48], L.A. Núñez[30], C. Oliveira[19], M. Palatka[32], J. Pallotta[9], S. Panja[32], G. Parente[79], T. Paulsen[38], J. Pawlowsky[38], M. Pech[32], J. Pękala[70], R. Pelayo[65], L.A.S. Pereira[23], E.E. Pereira Martins[39,7], J. Perez Armand[20], C. Pérez Bertolli[7,41], L. Perrone[56,48], S. Petrera[45,46], C. Petrucci[57,46], T. Pierog[41], M. Pimenta[72], M. Platino[7], B. Pont[80], M. Pothast[81,80], M. Pourmohammad Shahvar[61,47], P. Privitera[89], M. Prouza[32], A. Puyleart[87], S. Querchfeld[38], J. Rautenberg[38], D. Ravignani[7], M. Reininghaus[39], J. Ridky[32], F. Riehn[79], M. Risse[44], V. Rizi[57,46], W. Rodrigues de Carvalho[80], E. Rodriguez[7,41], J. Rodriguez Rojo[11], M.J. Roncoroni[7], S. Rossoni[43], M. Roth[41], E. Roulet[1], A.C. Rovero[4], P. Ruehl[44], A. Saftoiu[73], M. Saharan[80], F. Salamida[57,46], H. Salazar[64], G. Salina[51], J.D. Sanabria Gomez[30], F. Sánchez[7], E.M. Santos[20], E. Santos[32],

F. Sarazin[85], R. Sarmento[72], R. Sato[11], P. Savina[91], C.M. Schäfer[41], V. Scherini[56,48], H. Schieler[41], M. Schimassek[34], M. Schimp[38], F. Schlüter[41], D. Schmidt[39], O. Scholten[15,i], H. Schoorlemmer[80,81], P. Schovánek[32], F.G. Schröder[90,41], J. Schulte[42], T. Schulz[41], S.J. Sciutto[3], M. Scornavacche[7,41], A. Segreto[53,47], S. Sehgal[38], S.U. Shivashankara[76], G. Sigl[43], G. Silli[7], O. Sima[73,b], F. Simon[40], R. Smau[73], R. Šmída[89], P. Sommers[k], J.F. Soriano[86], R. Squartini[10], M. Stadelmaier[32], D. Stanca[73], S. Stanič[76], J. Stasielak[70], P. Stassi[36], S. Strähnz[39], M. Straub[42], M. Suárez-Durán[14], T. Suomijärvi[37], A.D. Supanitsky[7], Z. Svozilikova[32], Z. Szadkowski[71], A. Tapia[29], C. Taricco[63,52], C. Timmermans[81,80], O. Tkachenko[41], P. Tobiska[32], C.J. Todero Peixoto[18], B. Tomé[72], Z. Torrès[36], A. Travaini[10], P. Travnicek[32], C. Trimarelli[57,46], M. Tueros[3], M. Unger[41], L. Vaclavek[33], M. Vacula[33], J.F. Valdés Galicia[68], L. Valore[60,50], E. Varela[64], A. Vásquez-Ramírez[30], D. Veberič[41], C. Ventura[27], I.D. Vergara Quispe[3], V. Verzi[51], J. Vicha[32], J. Vink[83], J. Vlastimil[32], S. Vorobiov[76], C. Watanabe[26], A.A. Watson[c], A. Weindl[41], L. Wiencke[85], H. Wilczyński[70], D. Wittkowski[38], B. Wundheiler[7], B. Yue[38], A. Yushkov[32], O. Zapparrata[14], E. Zas[79], D. Zavrtanik[76,77], M. Zavrtanik[77,76]

[1] Centro Atómico Bariloche and Instituto Balseiro (CNEA-UNCuyo-CONICET), San Carlos de Bariloche, Argentina
[2] Departamento de Física and Departamento de Ciencias de la Atmósfera y los Océanos, FCEyN, Universidad de Buenos Aires and CONICET, Buenos Aires, Argentina
[3] IFLP, Universidad Nacional de La Plata and CONICET, La Plata, Argentina
[4] Instituto de Astronomía y Física del Espacio (IAFE, CONICET-UBA), Buenos Aires, Argentina
[5] Instituto de Física de Rosario (IFIR) – CONICET/U.N.R. and Facultad de Ciencias Bioquímicas y Farmacéuticas U.N.R., Rosario, Argentina
[6] Instituto de Tecnologías en Detección y Astropartículas (CNEA, CONICET, UNSAM), and Universidad Tecnológica Nacional – Facultad Regional Mendoza (CONICET/CNEA), Mendoza, Argentina
[7] Instituto de Tecnologías en Detección y Astropartículas (CNEA, CONICET, UNSAM), Buenos Aires, Argentina
[8] International Center of Advanced Studies and Instituto de Ciencias Físicas, ECyT-UNSAM and CONICET, Campus Miguelete – San Martín, Buenos Aires, Argentina
[9] Laboratorio Atmósfera – Departamento de Investigaciones en Láseres y sus Aplicaciones – UNIDEF (CITEDEF-CONICET), Argentina
[10] Observatorio Pierre Auger, Malargüe, Argentina
[11] Observatorio Pierre Auger and Comisión Nacional de Energía Atómica, Malargüe, Argentina
[12] Universidad Tecnológica Nacional – Facultad Regional Buenos Aires, Buenos Aires, Argentina
[13] University of Adelaide, Adelaide, S.A., Australia
[14] Université Libre de Bruxelles (ULB), Brussels, Belgium
[15] Vrije Universiteit Brussels, Brussels, Belgium
[16] Centro Federal de Educação Tecnológica Celso Suckow da Fonseca, Petropolis, Brazil
[17] Instituto Federal de Educação, Ciência e Tecnologia do Rio de Janeiro (IFRJ), Brazil
[18] Universidade de São Paulo, Escola de Engenharia de Lorena, Lorena, SP, Brazil
[19] Universidade de São Paulo, Instituto de Física de São Carlos, São Carlos, SP, Brazil
[20] Universidade de São Paulo, Instituto de Física, São Paulo, SP, Brazil
[21] Universidade Estadual de Campinas, IFGW, Campinas, SP, Brazil
[22] Universidade Estadual de Feira de Santana, Feira de Santana, Brazil
[23] Universidade Federal de Campina Grande, Centro de Ciencias e Tecnologia, Campina Grande, Brazil
[24] Universidade Federal do ABC, Santo André, SP, Brazil
[25] Universidade Federal do Paraná, Setor Palotina, Palotina, Brazil
[26] Universidade Federal do Rio de Janeiro, Instituto de Física, Rio de Janeiro, RJ, Brazil
[27] Universidade Federal do Rio de Janeiro (UFRJ), Observatório do Valongo, Rio de Janeiro, RJ, Brazil
[28] Universidade Federal Fluminense, EEIMVR, Volta Redonda, RJ, Brazil
[29] Universidad de Medellín, Medellín, Colombia
[30] Universidad Industrial de Santander, Bucaramanga, Colombia

[31] Charles University, Faculty of Mathematics and Physics, Institute of Particle and Nuclear Physics, Prague, Czech Republic
[32] Institute of Physics of the Czech Academy of Sciences, Prague, Czech Republic
[33] Palacky University, Olomouc, Czech Republic
[34] CNRS/IN2P3, IJCLab, Université Paris-Saclay, Orsay, France
[35] Laboratoire de Physique Nucléaire et de Hautes Energies (LPNHE), Sorbonne Université, Université de Paris, CNRS-IN2P3, Paris, France
[36] Univ. Grenoble Alpes, CNRS, Grenoble Institute of Engineering Univ. Grenoble Alpes, LPSC-IN2P3, 38000 Grenoble, France
[37] Université Paris-Saclay, CNRS/IN2P3, IJCLab, Orsay, France
[38] Bergische Universität Wuppertal, Department of Physics, Wuppertal, Germany
[39] Karlsruhe Institute of Technology (KIT), Institute for Experimental Particle Physics, Karlsruhe, Germany
[40] Karlsruhe Institute of Technology (KIT), Institut für Prozessdatenverarbeitung und Elektronik, Karlsruhe, Germany
[41] Karlsruhe Institute of Technology (KIT), Institute for Astroparticle Physics, Karlsruhe, Germany
[42] RWTH Aachen University, III. Physikalisches Institut A, Aachen, Germany
[43] Universität Hamburg, II. Institut für Theoretische Physik, Hamburg, Germany
[44] Universität Siegen, Department Physik – Experimentelle Teilchenphysik, Siegen, Germany
[45] Gran Sasso Science Institute, L'Aquila, Italy
[46] INFN Laboratori Nazionali del Gran Sasso, Assergi (L'Aquila), Italy
[47] INFN, Sezione di Catania, Catania, Italy
[48] INFN, Sezione di Lecce, Lecce, Italy
[49] INFN, Sezione di Milano, Milano, Italy
[50] INFN, Sezione di Napoli, Napoli, Italy
[51] INFN, Sezione di Roma "Tor Vergata", Roma, Italy
[52] INFN, Sezione di Torino, Torino, Italy
[53] Istituto di Astrofisica Spaziale e Fisica Cosmica di Palermo (INAF), Palermo, Italy
[54] Osservatorio Astrofisico di Torino (INAF), Torino, Italy
[55] Politecnico di Milano, Dipartimento di Scienze e Tecnologie Aerospaziali , Milano, Italy
[56] Università del Salento, Dipartimento di Matematica e Fisica "E. De Giorgi", Lecce, Italy
[57] Università dell'Aquila, Dipartimento di Scienze Fisiche e Chimiche, L'Aquila, Italy
[58] Università di Catania, Dipartimento di Fisica e Astronomia "Ettore Majorana", Catania, Italy
[59] Università di Milano, Dipartimento di Fisica, Milano, Italy
[60] Università di Napoli "Federico II", Dipartimento di Fisica "Ettore Pancini", Napoli, Italy
[61] Università di Palermo, Dipartimento di Fisica e Chimica "E. Segrè", Palermo, Italy
[62] Università di Roma "Tor Vergata", Dipartimento di Fisica, Roma, Italy
[63] Università Torino, Dipartimento di Fisica, Torino, Italy
[64] Benemérita Universidad Autónoma de Puebla, Puebla, México
[65] Unidad Profesional Interdisciplinaria en Ingeniería y Tecnologías Avanzadas del Instituto Politécnico Nacional (UPIITA-IPN), México, D.F., México
[66] Universidad Autónoma de Chiapas, Tuxtla Gutiérrez, Chiapas, México
[67] Universidad Michoacana de San Nicolás de Hidalgo, Morelia, Michoacán, México
[68] Universidad Nacional Autónoma de México, México, D.F., México
[69] Universidad Nacional de San Agustin de Arequipa, Facultad de Ciencias Naturales y Formales, Arequipa, Peru
[70] Institute of Nuclear Physics PAN, Krakow, Poland
[71] University of Łódź, Faculty of High-Energy Astrophysics,Łódź, Poland
[72] Laboratório de Instrumentação e Física Experimental de Partículas – LIP and Instituto Superior Técnico – IST, Universidade de Lisboa – UL, Lisboa, Portugal
[73] "Horia Hulubei" National Institute for Physics and Nuclear Engineering, Bucharest-Magurele, Romania
[74] Institute of Space Science, Bucharest-Magurele, Romania
[75] University Politehnica of Bucharest, Bucharest, Romania
[76] Center for Astrophysics and Cosmology (CAC), University of Nova Gorica, Nova Gorica, Slovenia
[77] Experimental Particle Physics Department, J. Stefan Institute, Ljubljana, Slovenia

PoS(ICRC2023)1099

[78] Universidad de Granada and C.A.F.P.E., Granada, Spain
[79] Instituto Galego de Física de Altas Enerxías (IGFAE), Universidade de Santiago de Compostela, Santiago de Compostela, Spain
[80] IMAPP, Radboud University Nijmegen, Nijmegen, The Netherlands
[81] Nationaal Instituut voor Kernfysica en Hoge Energie Fysica (NIKHEF), Science Park, Amsterdam, The Netherlands
[82] Stichting Astronomisch Onderzoek in Nederland (ASTRON), Dwingeloo, The Netherlands
[83] Universiteit van Amsterdam, Faculty of Science, Amsterdam, The Netherlands
[84] Case Western Reserve University, Cleveland, OH, USA
[85] Colorado School of Mines, Golden, CO, USA
[86] Department of Physics and Astronomy, Lehman College, City University of New York, Bronx, NY, USA
[87] Michigan Technological University, Houghton, MI, USA
[88] New York University, New York, NY, USA
[89] University of Chicago, Enrico Fermi Institute, Chicago, IL, USA
[90] University of Delaware, Department of Physics and Astronomy, Bartol Research Institute, Newark, DE, USA
[91] University of Wisconsin-Madison, Department of Physics and WIPAC, Madison, WI, USA

—

[a] Louisiana State University, Baton Rouge, LA, USA
[b] also at University of Bucharest, Physics Department, Bucharest, Romania
[c] School of Physics and Astronomy, University of Leeds, Leeds, United Kingdom
[d] now at Agenzia Spaziale Italiana (ASI). Via del Politecnico 00133, Roma, Italy
[e] Fermi National Accelerator Laboratory, Fermilab, Batavia, IL, USA
[f] now at Graduate School of Science, Osaka Metropolitan University, Osaka, Japan
[g] now at ECAP, Erlangen, Germany
[h] Max-Planck-Institut für Radioastronomie, Bonn, Germany
[i] also at Kapteyn Institute, University of Groningen, Groningen, The Netherlands
[j] Colorado State University, Fort Collins, CO, USA
[k] Pennsylvania State University, University Park, PA, USA

Acknowledgments

The successful installation, commissioning, and operation of the Pierre Auger Observatory would not have been possible without the strong commitment and effort from the technical and administrative staff in Malargüe. We are very grateful to the following agencies and organizations for financial support:

Argentina – Comisión Nacional de Energía Atómica; Agencia Nacional de Promoción Científica y Tecnológica (ANPCyT); Consejo Nacional de Investigaciones Científicas y Técnicas (CONICET); Gobierno de la Provincia de Mendoza; Municipalidad de Malargüe; NDM Holdings and Valle Las Leñas; in gratitude for their continuing cooperation over land access; Australia – the Australian Research Council; Belgium – Fonds de la Recherche Scientifique (FNRS); Research Foundation Flanders (FWO); Brazil – Conselho Nacional de Desenvolvimento Científico e Tecnológico (CNPq); Financiadora de Estudos e Projetos (FINEP); Fundação de Amparo à Pesquisa do Estado de Rio de Janeiro (FAPERJ); São Paulo Research Foundation (FAPESP) Grants No. 2019/10151-2, No. 2010/07359-6 and No. 1999/05404-3; Ministério da Ciência, Tecnologia, Inovações e Comunicações (MCTIC); Czech Republic – Grant No. MSMT CR LTT18004, LM2015038, LM2018102, CZ.02.1.01/0.0/0.0/16_013/0001402, CZ.02.1.01/0.0/0.0/18_046/0016010 and CZ.02.1.01/0.0/0.0/17_049/0008422; France – Centre de Calcul IN2P3/CNRS; Centre National de la Recherche Scientifique (CNRS); Conseil Régional Ile-de-France; Département Physique Nucléaire et Corpusculaire (PNC-IN2P3/CNRS); Département Sciences de l'Univers (SDU-INSU/CNRS); Institut Lagrange de Paris (ILP) Grant No. LABEX ANR-10-LABX-63 within the Investissements d'Avenir Programme Grant No. ANR-11-IDEX-0004-02; Germany – Bundesministerium für Bildung und Forschung (BMBF); Deutsche Forschungsgemeinschaft (DFG); Finanzministerium Baden-Württemberg; Helmholtz Alliance for Astroparticle Physics (HAP); Helmholtz-Gemeinschaft Deutscher Forschungszentren (HGF); Ministerium für Kultur und Wissenschaft des Landes Nordrhein-Westfalen; Ministerium für Wissenschaft, Forschung und Kunst des Landes Baden-Württemberg; Italy – Istituto Nazionale di Fisica Nucleare (INFN); Istituto Nazionale di Astrofisica (INAF); Ministero dell'Universitá e della Ricerca (MUR); CETEMPS Center of Excellence; Ministero degli Affari Esteri (MAE), ICSC Centro Nazionale di Ricerca in High Performance Computing, Big Data

and Quantum Computing, funded by European Union NextGenerationEU, reference code CN_00000013; México – Consejo Nacional de Ciencia y Tecnología (CONACYT) No. 167733; Universidad Nacional Autónoma de México (UNAM); PAPIIT DGAPA-UNAM; The Netherlands – Ministry of Education, Culture and Science; Netherlands Organisation for Scientific Research (NWO); Dutch national e-infrastructure with the support of SURF Cooperative; Poland – Ministry of Education and Science, grants No. DIR/WK/2018/11 and 2022/WK/12; National Science Centre, grants No. 2016/22/M/ST9/00198, 2016/23/B/ST9/01635, 2020/39/B/ST9/01398, and 2022/45/B/ST9/02163; Portugal – Portuguese national funds and FEDER funds within Programa Operacional Factores de Competitividade through Fundação para a Ciência e a Tecnologia (COMPETE); Romania – Ministry of Research, Innovation and Digitization, CNCS-UEFISCDI, contract no. 30N/2023 under Romanian National Core Program LAPLAS VII, grant no. PN 23 21 01 02 and project number PN-III-P1-1.1-TE-2021-0924/TE57/2022, within PNCDI III; Slovenia – Slovenian Research Agency, grants P1-0031, P1-0385, I0-0033, N1-0111; Spain – Ministerio de Economía, Industria y Competitividad (FPA2017-85114-P and PID2019-104676GB-C32), Xunta de Galicia (ED431C 2017/07), Junta de Andalucía (SOMM17/6104/UGR, P18-FR-4314) Feder Funds, RENATA Red Nacional Temática de Astropartículas (FPA2015-68783-REDT) and María de Maeztu Unit of Excellence (MDM-2016-0692); USA – Department of Energy, Contracts No. DE-AC02-07CH11359, No. DE-FR02-04ER41300, No. DE-FG02-99ER41107 and No. DE-SC0011689; National Science Foundation, Grant No. 0450696; The Grainger Foundation; Marie Curie-IRSES/EPLANET; European Particle Physics Latin American Network; and UNESCO.